Profiles and polarizations of the Balmer-α line from high-temperature hydrogen atoms in strong magnetic fields*

R. C. Isler†
Oak Ridge National Laboratory, Oak Ridge, Tennessee 37830
(Received 7 April 1976)

Energies and eigenstates are obtained for the $n = 2$ and $n = 3$ levels of hydrogen atoms moving in strong magnetic fields. The Hamiltonian of the system includes the interaction with the Lorentz field, $\vec{E} = \vec{v} \times \vec{B}$, as well as the magnetic interaction, $-\vec{\mu} \cdot \vec{B}$. These results are utilized together with the Doppler shifts in order to obtain profiles and polarizations of the Balmer-α line in tokamak-like environments under the assumption that the velocity distributions are Maxwellian.

I. INTRODUCTION

Programs are currently in operation in several laboratories to determine the temperatures of tokamak-produced plasmas from Doppler-broadened spectral lines. The plasmas are characterized by high kinetic temperatures, low densities, and strong magnetic fields which have typical values of 1–2 keV, 4×10^{13} cm^{-3}, and 2×10^{4} G at the center of the discharge. Although the dominant contribution to the lines of hydrogen is expected to originate in a relatively cool, narrow region near the outside of the plasma, where the concentration of neutral particles is highest, experiments show that the wings of the Balmer lines may be quite broad due to the presence of fast atoms which are formed through charge exchange with energetic protons.[1] Thus detailed measurements of the profiles of the Balmer lines may reveal information from the interior as well as from the exterior of the plasma.[2]

The present calculation has been undertaken in order to determine the extent to which mechanisms other than Doppler broadening can affect the shape of the Balmer-α line. It appears that the most important secondary influences which require consideration are the Zeeman effect and the translational Stark effect which arises from the Lorentz field,

$$\vec{E} = \vec{v} \times \vec{B} . \tag{1}$$

Galushkin[3] has investigated these interactions for certain very specialized or limiting cases but has not computed complete profiles of any of the lines of hydrogen. Owing to the low density of charged particles, collisional Stark broadening is negligible for the plasmas treated here.

II. SPECTRAL SHIFTS

The lifetimes of the states of the $n = 3$ level are short enough for it to be a good approximation to consider a radiating atom as experiencing constant external fields and therefore emitting a single frequency. We employ a coordinate system in which the magnetic field is oriented in the z direction and observations are made in the x direction; the frequency detected from a transition between two states k and j is given by the expression

$$\nu_{kj} = (E_0 + \Delta E_{kj})(1 + v_r \cos\phi/c)/h , \tag{2}$$

where E_0 is the energy in the absence of any external field, ΔE_{kj} is the difference in the shifts between the initial and the final states in the presence of the field, v_r is the magnitude of atomic velocity perpendicular to $\vec{B}$, and ϕ is the angle that the velocity vector of the moving atom makes with the x axis. The perturbed energies ΔE_{kj} are obtained by diagonalizing the matrix representation of the Hamiltonian,

$$\mathcal{H}' = e\vec{E} \cdot \vec{r} + (\beta B/\hbar) L_z . \tag{3}$$

Because the strong magnetic field effectively decouples the spin and orbital angular momenta of the atomic electron it is most convenient to use an $|lm\rangle$ basis set for calculating matrix elements.

An extra energy, $\pm\beta B$, must be added to the eigenvalues of $\mathcal{H}'$ in order to account for the interaction of the magnetic moment of the electron with the external field. These terms cancel in the shifts of the spectral lines, since transitions are considered to take place only between states which have the same quantum number m_s.

It is important to point out that the present calculation becomes more exact as larger magnetic fields and higher temperatures are considered. The fine-structure interaction, which is omitted from Eq. (3), is responsible for a separation of 0.20 Å in the extreme components of the Balmer-α line, and this splitting may exceed the broadening caused by external fields when B and kT are small.

After substituting Eq. (1) into Eq. (3) the Hamiltonian can be written

$$\mathcal{H}' = \tfrac{1}{2} e v_r B(\tau^* r^- - \tau r^+) + (\beta B/\hbar) L_z , \qquad (4)$$

where $\tau = ie^{-i\phi}$ and $r^{\pm}$ are spherical components of the vector $\vec{r}$.

Tables I–III list the eigenfunctions and the eigenvectors which are obtained for the $n=2$ and the $n=3$ states of hydrogen after diagonalizing the matrix of the perturbation. The notation employed in the tables is the following:

$$\epsilon = 3ea_0 v_r B , \quad \gamma = \beta B ,$$

$$q_0 = (\gamma^2 + \epsilon^2)^{1/2} , \quad q_1 = (4\gamma^2 + 9\epsilon^2)^{1/2} .$$

III. LINE SHAPES AND POLARIZATIONS

Under the coronal conditions which exist in tokamak-produced plasmas the concentration of atoms in the upper state of a transition is determined by the ratio of the probabilities for excitation and for radiative decay. Collisions of electrons with hydrogen atoms in the ground state provide the most efficient means for excitation. The rates for populating the S, P, and D levels all vary, however. If the collisions are isotropic (no difference between $T_{\parallel}$ and $T_{\perp}$ for the electrons[4]) the rate of excitation of an excited state, k, is

$$R_k = n_0 n_e \sum_{l,m} |a_{klm}|^2 r_{kl} , \qquad (5)$$

where r_{kl} is the rate coefficient for populating a given angular momentum state and a_{klm} is the coefficient of the basis vector $|lm\rangle$. It is assumed in the present calculations that the rate coefficients are independent of the azimuthal quantum number m.

The lifetime for radiative decay is expressed as

$$t_k = A_k^{-1} = \left(\sum_{l,m} \frac{|a_{klm}|^2}{t_{kl}} \right)^{-1} . \qquad (6)$$

In addition to the energy of an excited state being a function of v_r, Eqs. (5) and (6) show that the rates of excitation and the lifetimes are also dependent upon the speed of the moving atom through the coefficients a_{klm}.

The total intensity emitted at a wavelength $\Delta\lambda$ from the unshifted line by the collection of radiating atoms is obtained for a given component by weighting the intensity from a single atom with a Maxwellian distribution and integrating over the independent coordinates. After changing the velocity distribution in v_r and ϕ to a distribution in v_r and $\Delta\lambda$ with the aid of the Jacobian $v_r \lambda_0 \sin\phi / c$, we can write

$$I_{k,j}(\Delta\lambda) = K \int_{v_{\min}}^{\infty} |\langle k | \vec{\epsilon} \cdot \vec{r} | j \rangle|^2 \tau_k R_k \times \exp\left(-\frac{M v_r^2}{2kT}\right) \frac{dv_r}{\sin\phi} , \qquad (7)$$

TABLE I. Energy shifts and coefficients of the $|nlm\rangle$ basis set of the eigenstates of the Zeeman and the translational Stark effects. All coefficients must be divided by q_1^2 in order to normalize the eigenstates to unity.

n	l	m	ΔE / q_1	$-q_1$	$\frac{1}{2}q_1$	$-\frac{1}{2}q_1$	0	0
3	0	0	$3\sqrt{3}\,\epsilon^2$	$3\sqrt{3}\,\epsilon^2$	$4\sqrt{3}\,\epsilon\gamma$	$4\sqrt{3}\,\epsilon\gamma$	$\frac{1}{3}\sqrt{2}\,(8\gamma^2 - 9\epsilon^2)$	$\frac{1}{3}q_1^2$
3	1	1	$\frac{3}{2}\tau\epsilon(2\gamma + q_1)$	$\frac{3}{2}\tau\epsilon(2\gamma - q_1)$	$\frac{1}{2}\tau(4\gamma^2 - 9\epsilon^2 + 2\gamma q_1)$	$\frac{1}{2}\tau(4\gamma^2 - 9\epsilon^2 - 2\gamma q_1)$	$-3\sqrt{6}\,\tau\gamma\epsilon$	0
3	1	−1	$\frac{3}{2}\tau^*\epsilon(2\gamma - q_1)$	$\frac{3}{2}\tau^*\epsilon(2\gamma + q_1)$	$\frac{1}{2}\tau^*(4\gamma^2 - 9\epsilon^2 - 2\gamma q_1)$	$\frac{1}{2}\tau^*(4\gamma^2 - 9\epsilon^2 + 2\gamma q_1)$	$-3\sqrt{6}\,\tau^*\gamma\epsilon$	0
3	2	0	$-3\sqrt{3}\,\epsilon^2/2\sqrt{2}$	$-3\sqrt{3}\,\epsilon^2/2\sqrt{2}$	$-\sqrt{6}\,\epsilon\gamma$	$-\sqrt{6}\,\epsilon\gamma$	$-\frac{1}{6}(8\gamma^2 - 9\epsilon^2)$	$\frac{2}{3}\sqrt{2}\,q_1^2$
3	2	2	$\frac{1}{4}\tau^2(8\gamma^2 + 9\epsilon^2 + 4\gamma q_1)$	$\frac{1}{4}\tau^2(8\gamma^2 + 9\epsilon^2 - 4\gamma q_1)$	$-\frac{3}{2}\tau^2\epsilon(2\gamma + q_1)$	$-\frac{3}{2}\tau^2\epsilon(2\gamma - q_1)$	$9\sqrt{3}\,\tau^2\epsilon^2/2\sqrt{2}$	0
3	2	−2	$\frac{1}{4}(\tau^*)^2(8\gamma^2 + 9\epsilon^2 - 4\gamma q_1)$	$\frac{1}{4}(\tau^*)^2(8\gamma^2 + 9\epsilon^2 + 4\gamma q_1)$	$-\frac{3}{2}(\tau^*)^2\epsilon(2\gamma - q_1)$	$-\frac{3}{2}(\tau^*)^2\epsilon(2\gamma + q_1)$	$9\sqrt{3}\,(\tau^*)^2\epsilon^2/2\sqrt{2}$	0

TABLE II. Energy shifts and coefficients of the $|nl\,m\rangle$ basis set of the eigenstates of the Zeeman and the translational Stark effects. All coefficients must be divided by q_1 to normalize the eigenstates to unity.

n	l	m \ ΔE	0	$\frac{1}{2}q_1$	$-\frac{1}{2}q_1$
3	1	0	2γ	$3\epsilon/\sqrt{2}$	$3\epsilon/\sqrt{2}$
3	2	1	$-3\tau\epsilon/\sqrt{2}$	$\frac{1}{2}\tau(2\gamma+q_1)$	$\frac{1}{2}\tau(2\gamma-q_1)$
3	2	−1	$-3\tau^*\epsilon/\sqrt{2}$	$\frac{1}{2}\tau^*(2\gamma-q_1)$	$\frac{1}{2}\tau^*(2\gamma+q_1)$

in which $\sin\phi$ is obtained from the relationship

$$\cos\phi = -\frac{\lambda_0}{v_r}\left(\frac{c\Delta\lambda_{k,j}}{\lambda_0^2}+\frac{\Delta E_{k,j}}{h}\right). \tag{8}$$

The lower limit of the integral of Eq. (7) is the minimum velocity that can contribute to the shift $\Delta\lambda$; it is determined by the conditions for which $\sin\phi = 0$.

Equation (7) is solved by numerical quadrature in order to obtain $I_{k,j}(\Delta\lambda)$. The integration, which employs only the trapezoidal rule, is begun at an upper limit that is chosen as $[3+\Delta\lambda(\text{Å})]\bar{v}_r$, where $\bar{v}_r$ is the average velocity of the atoms at the temperature of interest, and the lower limit is approached in increments of Δv_r which become successively smaller as $\sin\phi$ approaches zero. Corroborations of the results have been obtained by performing a second type of numerical integration in the limit as the Bohr magneton approaches zero. In this limit $I_{k,j}(\Delta\lambda)$ can also be evaluated easily by an integration over a finite interval in the variable ϕ. Differences between the results obtained by the two methods are less than 2%, so that the numerical techniques employed in solving Eq. (7) appear to be satisfactory in view of the quality of the experimental data that can be currently obtained.

The dependence of hydrogenic profiles upon the temperature of the electrons, T_e, is implicit in the rate coefficients which appear in Eq. (7). Although the rate for exciting the P state from the ground state is always larger than the rates for exciting the S and D states, the latter two processes are relatively more important at low temperatures. In general, the local temperature of the electrons exceeds the temperature of the atoms, although the reverse situation may hold for any hot component of the atomic distribution function in the outer regions of the plasma. Accordingly, several relative values of the rates of excitation have been investigated in calculating the profiles and the polarizations of the Balmer-α line. Estimates of the variations expected among these rates have been made by assuming that they scale according to Vainstein's Born-approximation calculations[5] of the cross sections at energies which are equal to kT_e.

Line shapes which include radiation that is polarized both perpendicular and parallel to the magnetic field are shown in Fig. 1 for an atomic temperature of 400 eV and a field strength of 20 kG. Profiles 1(b) and 1(c) have been computed for cross sections that correspond to electronic energies of 60 and 800 eV, respectively. Profile 1(d) represents the limit for excitation by electrons of very high energy; only the P states are excited in this case.

Previous calculations that incorporated only the Doppler and the translational Stark effects[6] tended to produce profiles having depressions in the center of about 10% (or 20% if only the component polarized perpendicular to $\vec{B}$ was considered). The inclusion of the Zeeman effect and the concommitant dependence of the eigenstates upon v_r leads to

TABLE III. Energy shifts and coefficients of the $|nlm\rangle$ basis set of the eigenstates of the Zeeman and the translational Stark effects. All coefficients must be divided by q_0 in order to normalize the eigenstates to unity.

n	l	m \ ΔE	0	$+q_0$	$-q_0$	0
2	0	0	γ	$\epsilon/\sqrt{2}$	$\epsilon/\sqrt{2}$	0
2	1	1	$-\tau\epsilon/\sqrt{2}$	$\frac{1}{2}\tau(\gamma+q_0)$	$\frac{1}{2}\tau(\gamma-q_0)$	0
2	1	−1	$-\tau^*\epsilon/\sqrt{2}$	$\frac{1}{2}\tau^*(\gamma-q_0)$	$\frac{1}{2}\tau^*(\gamma+q_0)$	0
2	1	0	0	0	0	q_0

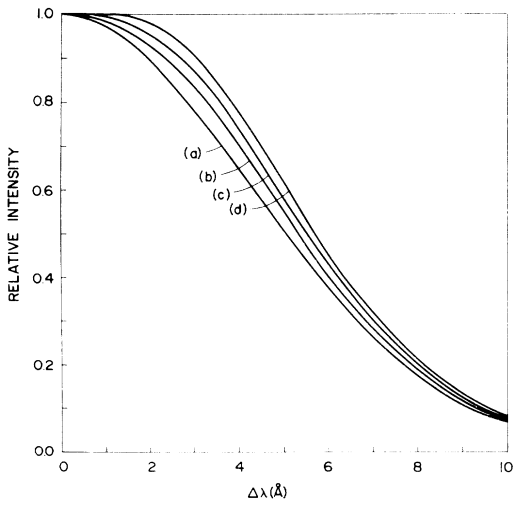

FIG. 1. Profiles of the Balmer-α line for an atomic temperature of 400 eV and a magnetic field of 20 kG. Curve (a) is a pure Doppler profile. Curves (b), (c), and (d) include the Zeeman and the translational Stark broadening and, respectively, correspond to excitation of the S, P, and D levels in the ratios 0.1:1.0:0.1, 0.05:1.0:0.04, 0:1.0:0.

profiles that are somewhat flatter than pure Doppler line shapes near the center but which exhibit central depressions of less than 1%. At values of $\Delta\lambda$ within 1.0 Å there are small fluctuations of the order of 3%; these are not shown in Fig. 1. At a temperature of 400 eV the half width at half-maximum intensity varies from 1.05 to 1.13 times the pure Doppler width, the largest deviation occurring when the rates for excitation of the S and the D states are assumed to be zero. The deviations are smaller, of course, at lower temperatures; the Doppler half-widths $\Delta\lambda_D$ and the half-widths that include the broadening from the external field are listed in Table IV for several atomic temperatures. Rates of excitation have been chosen to simulate conditions for which the energy of the electrons is approximately equal to $2kT$.

The polarizations of the hydrogen lines, as well as the widths, are functions of the temperature and the rates of excitation. The polarization is defined as

$$P=(I_{\parallel}-I_{\perp})/(I_{\parallel}+I_{\perp}),$$

where $I_{\parallel}$ and $I_{\perp}$ are the intensities of radiation emitted with electric vectors parallel and perpendicular to the magnetic field $\vec{B}$. This quantity is plotted in Fig. 2 as a function of $\Delta\lambda/\Delta\lambda_D$ for several atomic temperatures and for rates of excitation which again are appropriate to electronic energies of about $2kT$. It may at first appear surprising that the line should be polarized at all, since we have postulated isotropic excitation which is independent of the magnetic quantum number. But owing to the mixing of the pure angular momentum states by the Lorentz field, the several states of the $n=3$ level have very different lifetimes and the assumptions of unequal rates of excitation and the existence of coronal equilibrium therefore imply that the populations also differ. Hence the occurrence of strongly polarized emission should not be unexpected. At low temperatures, where the bulk of the atoms have small velocities, the eigenstates of the operator can be nearly represented as states of pure angular momentum, and the overall polarization should be small. This effect is seen in Fig. 2 at small values of $\Delta\lambda$ in the curve which pertains to $kT=16$ eV. However, the wings of the line result only from atoms that have relatively large velocities and the polarization is subsequently large there. At higher temperatures the line is strongly polarized near the center and the increase in the wings is not so dramatic within the range of $2\Delta\lambda_D$.

The dependence of polarization upon the relative rates of excitation is demonstrated in Fig. 3 for a fixed atomic temperature of 400 eV. The polarization is largest if excitation of the S and D states is negligible, and gradually diminishes as these two rates become more important. In the limit of uniform excitation the polarization actually changes sign and becomes positive. Thus the Balmer-α line should be more highly polarized if it is emitted from a region of the plasma where the temperature of the electrons is high. This fact may prove useful in determining where the hydrogenic lines are actually produced within the discharge, since many experiments are not constructed with the option of obtaining spatial resolution through an Abel inversion of data acquired by observing the emission along several chords. However, full exploitation of this effect would obviously require a treatment of the rates of excitation which includes the contributions from cascades and possibly from recombination.

TABLE IV. Half width at half-maximum intensity of Doppler profiles, $\Delta\lambda_D$, and profiles which include broadening by the external fields, $\Delta\lambda_{1/2}$. The excitation coefficients are appropriate to electronic energies that are approximately equal to $2kT$.

T (eV)	$\Delta\lambda_D$ (Å)	$\Delta\lambda_{1/2}$ (Å)	Excitation coefficients S	P	D
16	1.01	1.01	0.15	1.0	0.09
80	2.26	2.40	0.08	1.0	0.06
400	5.06	5.55	0.05	1.0	0.04
1600	10.12	10.63	0.04	1.0	0.03

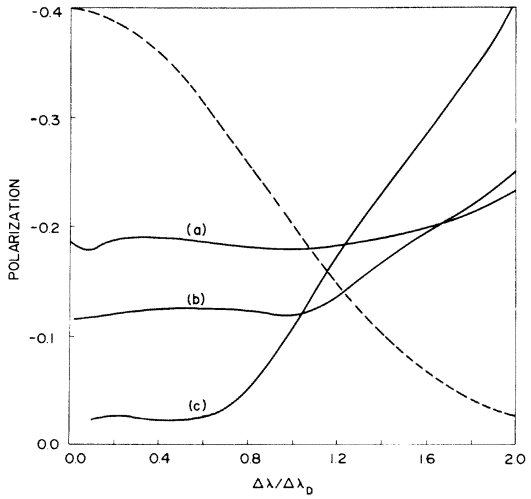

FIG. 2. Polarization of the Balmer-α line as a function of reduced wavelength. (a) $kT=400$ eV, rates of $S:P:D$ excitation are 0.05:1.0:0.04; (b) $kT=80$ eV, rates of $S:P:D$ excitation are 0.1:1.0:0.07; (c) $kT=16$ eV, rates of $S:P:D$ excitation are 0.15:1.0:0.09. The dashed line is a Doppler profile.

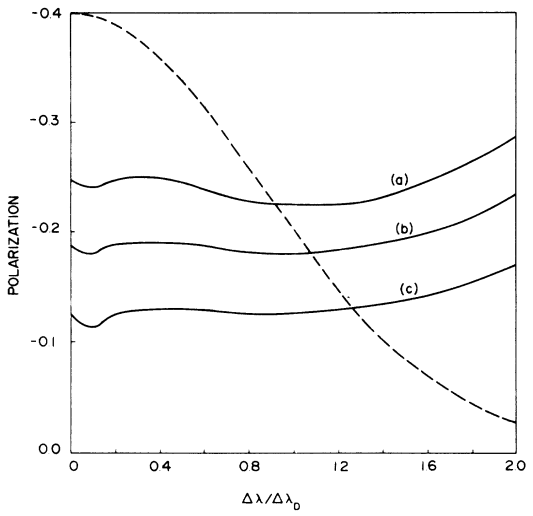

FIG. 3. Polarization of the Balmer-α line as a function of reduced wavelength for an atomic temperature of 400 eV. Rates of $S:P:D$ excitation are (a) 0.0:1.0:0.0, (b) 0.05:1.0:0.04, (c) 0.1:1.0:0. The dashed line is a Doppler profile.

IV. SUMMARY

Efforts have been made to evaluate the extent to which the combined Zeeman and translational Stark effects may cause profiles of the Balmer-α line to deviate from a pure Doppler shape in tokamak-produced environments. The differences are found to be largest near the center of the line, and corrections to the half-width are less than 10% for most cases of interest. At temperatures below about 60 eV these corrections are, in fact, less than the intrinsic fine structure of 0.2 Å.

The polarization of the Balmer-α line is strongly dependent upon the rates at which the different angular momentum states are excited. This result may prove useful in correlating the electronic and atomic temperatures at various depths within the plasma.

ACKNOWLEDGMENT

The assistance of K. A. French with the numerical computations for this study has been greatly appreciated.

---

*Research sponsored by the U.S. Energy Research and Development Administration under contract with the Union Carbide Corporation.

†On leave from the Dept. of Physics, Univ. of Florida, Gainesville, Fla. 32605.

[1]R. V. Neidigh, J. F. Clarke, J. R. McNally, Jr., and D. J. Sigmar, Bull. Am. Phys. Soc. 18, 1308 (1973).

[2]D. J. Sigmar, J. F. Clarke, R. V. Neidigh, and K. L. Vander Sluis, Phys. Rev. Lett. 33, 1376 (1974).

[3]Yu. I. Galushkin, Astron. Zh. 47, 375 (1969) [Sov. Astron.-AJ 14, 301 (1970)].

[4]Isotropic excitation produces line shapes that are symmetric around $\Delta\lambda=0$. Anisotropic excitation can lead to asymmetries, because the relative phases of certain states in the basis set may be opposite for pairs of eigenstates which have equal but opposite values of ΔE_k.

[5]B. L. Moiseiwitsch and S. J. Smith, NSRDS-NBS No. 25 (U.S. GPO, Washington, D. C., 1969).

[6]R. C. Isler, Bull. Am. Phys. Soc. 20, 1227 (1975).